

QUANTIFYING THE IMPACT OF COSMOLOGICAL PARAMETER UNCERTAINTIES ON STRONG LENSING MODELS WITH AN EYE TOWARD THE FRONTIER FIELDS

MATTHEW B. BAYLISS^{1,2}, KEREN SHARON³, AND TRACI JOHNSON³*Draft version March 27, 2015*

ABSTRACT

We test the effects of varying the cosmological parameter values used in the strong lens modeling process for the six Hubble Frontier Fields (HFF) galaxy clusters. The standard procedure for generating high fidelity strong lens models includes careful consideration of uncertainties in the output models that result from varying model parameters within the bounds of available data constraints. It is not, however, common practice to account for the effects of cosmological parameter value uncertainties. The convention is to instead use a single fiducial “concordance cosmology” and generate lens models assuming zero uncertainty in cosmological parameter values. We find that the magnification maps of the individual HFF clusters vary significantly when lens models are computed using different cosmological parameter values taken from recent literature constraints from space- and ground-based experiments. Specifically, the magnification maps have average variances across the best fit models computed using different cosmologies that are comparable in magnitude to – and as much as $2.5\times$ larger than – the model fitting uncertainties in each best fit model. We also find that estimates of the mass profiles of the cluster cores themselves vary only slightly when different input cosmological parameters are used. We conclude that cosmological parameter uncertainty is a non-negligible source of uncertainty in lens model products for the HFF clusters, and that it is important that current and future work which relies on precision strong lensing models take care to account for this additional source of uncertainty.

Subject headings: gravitational lensing: strong — cosmology: observations — cosmological parameters — galaxies: high-redshift

1. INTRODUCTION

Strong gravitational lensing enhances the best-available observational facilities by naturally zooming in on the distant universe. Massive galaxy clusters are the most effective “natural telescopes” available to us, because they provide high-magnification over relatively large regions of the sky (~ 1 sq. arcmin). We are entering a new era in which strong lensing is transitioning from a niche field into an important piece in the toolkit of observational cosmologists. Perhaps the most publicized evidence of this transition is the *Hubble* Frontier Fields (HFF)⁴ initiative. The HFF are specifically designed to exploit the magnification from strong lensing by clusters of galaxies. The HFF, in particular, are intended to probe galaxy populations at high redshift that are 10 or more times fainter than the faintest sources detected in existing deep field observations, and will yield new insights into galaxy evolution studies at high redshift, and the properties of galaxies during the epoch of re-ionization.

Strong lensing holds tremendous potential for enabling studies of the distant universe, but using strong lens models introduces new sources of systematic uncertainty (e.g., Coe et al. 2013; Tagore & Keeton 2014; Zitrin et al. 2014). To enable prompt use of new and up-

coming HFF data to constrain the properties of galaxies in the background universe several independent teams were tasked with generating lens models using existing archival *Hubble* imaging of the HFF (Bradač et al. 2005, 2009; Liesenborgs et al. 2006; Jullo et al. 2007; Jullo & Kneib 2009; Merten et al. 2009; Johnson et al. 2014; Richard et al. 2014). The primary lens model products are the convergence (κ) and shear (γ) maps, which can be used to construct magnification maps for sources at a given redshift, z_s . These models are a starting point, and are publicly available⁵; the first wave of models incorporating new HFF observations are now appearing (Ishigaki et al. 2014; Jauzac et al. 2014a,b).

The typical approach for generating strong lensing models is to assume a single fiducial set of cosmological parameters, for example a flat Λ cold dark matter (Λ CDM) cosmology with $H_0 = 70$ km s⁻¹ Mpc⁻¹, matter density $\Omega_M = 0.3$, and $\Omega_\Lambda = (1 - \Omega_M)$. However, as the precision of the strong lensing models improve they should, at some point, become sensitive to the uncertainties in these input cosmological parameter values. In this Letter we investigate how strong lensing model uncertainties vary with different input cosmological parameter values. We take the input parameter values from three recent experiments – the Wilkinson Microwave Anisotropy Probe (WMAP; Hinshaw et al. 2013), the South Pole Telescope (SPT; Reichardt et al. 2013), and the *Planck* satellite (Planck Collaboration et al. 2014) – in addition to the fiducial “concordance cosmology”. The exact cosmological parameter values that we use are summarized in Table 1 with more details available from the

mbayliss@cfa.harvard.edu

¹ Department of Physics, Harvard University, 17 Oxford St., Cambridge, MA 02138² Harvard-Smithsonian Center for Astrophysics, 60 Garden St., Cambridge, MA 02138³ Department of Astronomy, the University of Michigan, 500 Church St. Ann Arbor, MI 48109⁴ <http://www.stsci.edu/hst/campaigns/frontier-fields/>⁵ <http://archive.stsci.edu/prepds/frontier/lensmodels/>

TABLE 1
COSMOLOGICAL PARAMETER CONSTRAINTS FROM THE LITERATURE

Source	Ω_M^a	H_0 (km s $^{-1}$)	Reference
fiducial “concordance cosmology”	0.300	70	—
Planck 2013+WP+hL+BAO	0.308 ± 0.01	67.8 ± 0.8	Planck Collaboration et al. (2014)
WMAP-9+eCMB+H $_0$ +BAO	0.286 ± 0.01	69.3 ± 0.8	Hinshaw et al. (2013)
SPT Clusters+WMAP+SNe	0.255 ± 0.016	71.6 ± 1.5	Reichardt et al. (2013)

^a We restrict ourselves to cosmologies that assume a flat geometry, so that $\Omega_\Lambda = 1 - \Omega_M$; see the references in column 4 for more details.

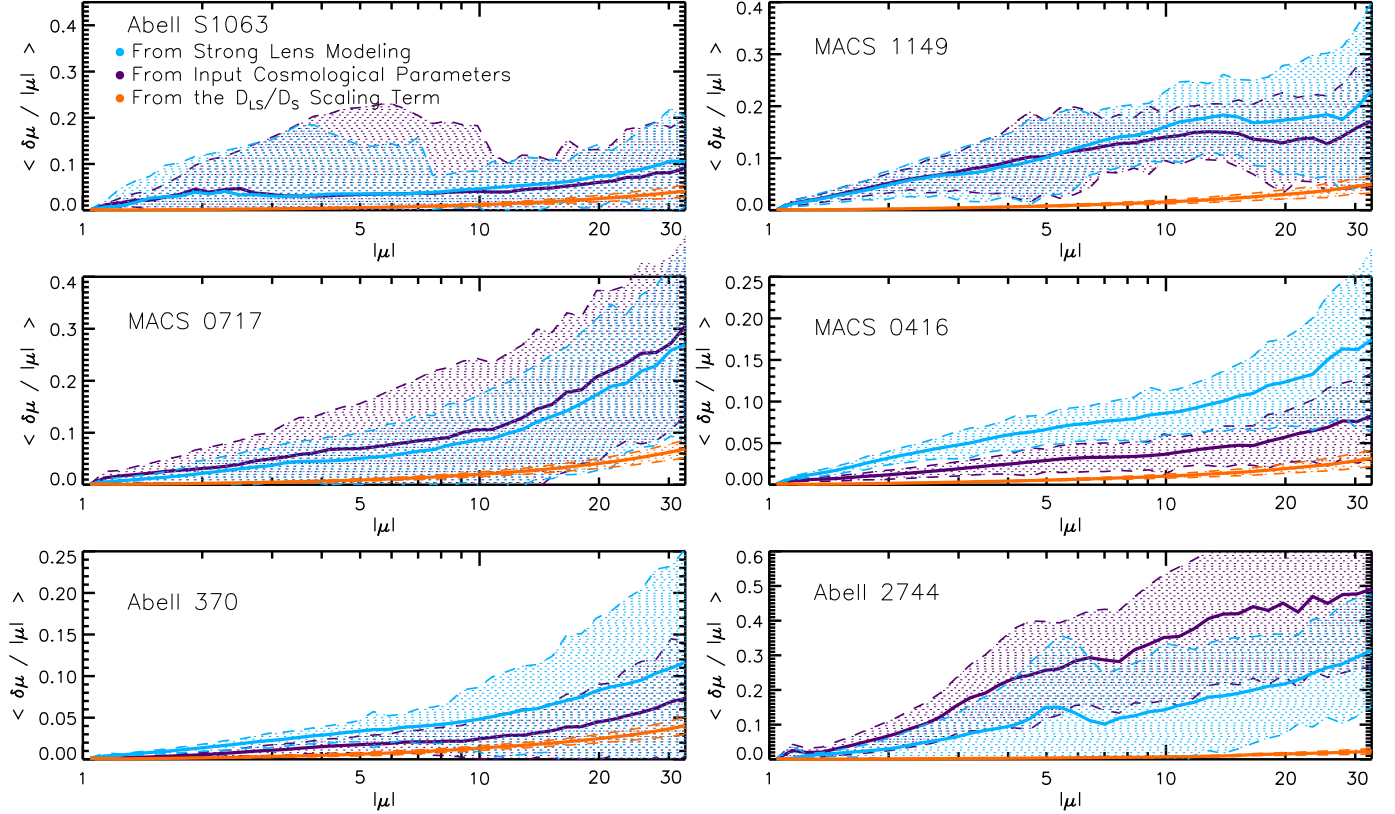


FIG. 1.— The fractional magnification uncertainty of individual pixels as a function of the mean magnification value in each pixel for each of the six HFF clusters for sources at $z = 3$. The solid lines indicate the median fractional uncertainty of all pixels of a given magnification value, and the shaded regions indicate the 1σ spread. Blue represents the “statistical” uncertainties from the MCMC minimization over lens model parameters; purple represents the uncertainties that result from varying the input cosmological parameter values; and orange represents the uncertainties that are imposed via the uncertainty in the D_{LS}/D_S scaling term that is applied to the κ and γ maps to a source-plane at $z = 3$.

references therein.

2. LENS MODELS AND COSMOLOGICAL PARAMETERS

The cosmological parameters that impact the lens modeling process are those that relate directly to computing cosmological distances, i.e., the Hubble constant, H_0 and the matter density Ω_M . Here we restrict ourselves to flat cosmologies, so that the vacuum energy density, Ω_Λ , is $1 - \Omega_M$. These parameters influence gravitational lensing via the angular diameter distances to the lens, d_l , the source, d_s , and between the lens and the source, d_{ls} (e.g., Fukugita et al. 1992; Schneider et al. 1992); different values of H_0 and Ω_M correspond to different geometric distances between a gravitational lensing potential and a background source.

In the gravitational lens equation,

$$\vec{\beta} = \vec{\theta} - \vec{\alpha} \quad (1)$$

the deflection angle, $\vec{\alpha}$, is the difference between the observed and true positions on the sky – $\vec{\theta}$ and $\vec{\beta}$, respectively – of a background source. The deflection angle can be written in terms of the convergence, $\kappa(\vec{\theta})$, which is defined as the surface mass density of the lensing potential in units of the critical surface mass density, Σ_{crit} .

$$\nabla \cdot \vec{\alpha} = 2\kappa(\vec{\theta}) \quad (2)$$

where,

$$\kappa(\vec{\theta}) = \frac{\Sigma(\vec{\theta})}{\Sigma_{crit}} \quad (3)$$

The critical surface mass density is the surface mass density that is sufficient for a gravitational lens at a given

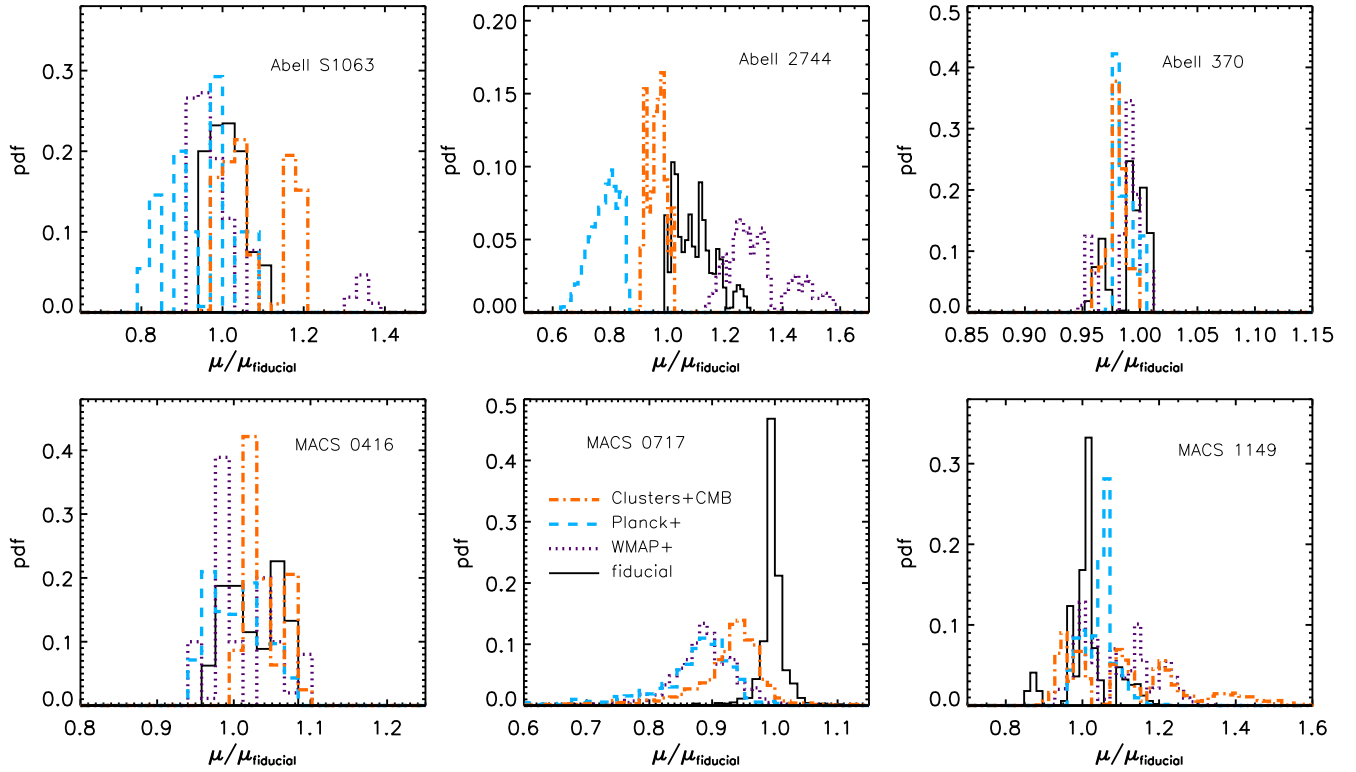


FIG. 2.— The distribution of magnification values of pixels in a random position in each of the six HFF lens models, separated by input cosmology. At each random position we normalize the magnification values of all pixels in a box of size 9×9 pixels ($4.5''$ to a side) by the magnification value of the central pixel in the best-fit fiducial cosmology. There are clear systematic shifts in the distribution of pixel magnification values across a statistical sampling of models when different input cosmologies are used. The magnitude and direction of those shifts change w/ position across each cluster field; these plots of a random region in each HFF field simply serve to illustrate that there are systematic shifts in magnification that result from the input cosmology.

redshift, z_l , to produce multiple images of a background source at a given redshift, z_s :

$$\Sigma_{crit} = \frac{c}{4\pi G} \frac{d_s(z_s)}{d_l(z_l)d_{ls}(z_l, z_s)}. \quad (4)$$

Formulated this way one can think of the gravitational deflection angle as a function of two terms. The first, $\Sigma(\vec{\theta})$, describes the surface mass distribution of the lensing potential, and the second, Σ_{crit} , depends on the source-lens-observer geometry. The second term is sensitive to cosmological parameters, as values of H_0 and Ω_M result in different values of the angular diameter distance to the lens, to the source, and between the lens and source.

3. QUANTIFYING THE COSMOLOGICAL IMPACT ON LENS MODELS

Our goal is to quantify the degree to which varying cosmological parameter values within their current best-constraints affects measurements of background sources that rely on strong lensing models. We narrow our analysis to the HFF because these six clusters are among the best studied lenses with an emphasis on their use as precision cosmic telescopes. There are two ways in which the input cosmological parameters will – via the distance term in Σ_{crit} – influence measurements that rely on lens model products. Firstly, the input cosmology used when modeling the strong lensing potential determines basic physical quantities, most notably the rela-

tionship between angular scale on the sky and physical scale in the lens/source planes (e.g., kpc/"). Secondly, the lensing model products are computed for a single source-plane redshift – for example the Johnson et al. (2014) lens models use $z_s = 9$ – and those products must be scaled to the source redshifts of specific individual background galaxies. We investigate how each of these effects induce variations in the strong lensing magnification maps.

We restrict our analysis to the lens models of Johnson et al. (2014), which are generated using the **Lenstool** software (Jullo et al. 2007); we are explicitly not sampling all sources of uncertainty in the lens modeling process. Understanding the “true” total lens model uncertainties is the subject of ongoing work across the strong lensing community; this Letter is one piece of that larger effort. We do not account for potential systematic uncertainty due to uncorrelated line-of-sight structure (Bayliss et al. 2014a; D’Aloisio et al. 2014). The magnitude of such line-of-sight effects is not well-understood, and including it in the modeling would require significant observational follow-up and code development (McCully et al. 2014).

3.1. Impact of Cosmological Uncertainty On Magnification Maps

The first test that we perform is designed to assess the degree to which the input cosmological parameters affect strong lensing models. We do this by modeling each cluster using four different cosmologies (Table 1) taken from

the literature to span the range of the current best constraints for H_0 and Ω_M in a flat Λ CDM cosmology. We use identical observational constraints and lens model assumptions as Johnson et al. (2014), and generate models for background source redshifts of $z_s = 3$. For each lens model of each cluster we generate maps that assign magnification values to the pixelated sky, with the pixelation of the maps preserved across all models of a given cluster.

A family of lens models for each cluster in each cosmology is generated from lens model parameter values drawn from the MCMC minimization (see e.g., Sharon et al. 2012; Bayliss et al. 2014b; Johnson et al. 2014; Sharon et al. 2014). For each cluster in each cosmology this provides a statistical range of lens models spanning the 68% confidence region in the MCMC parameter space as traced by χ^2 . From the family of models generated using the fiducial cosmology we measure the $1-\sigma$ uncertainty in the magnification of each pixel as half of the full range spanned across the models that sample the 68% confidence region. We call these uncertainties “statistical uncertainties” throughout this letter. We then compute the root mean squared (RMS) scatter in the magnification values for each pixel across the best-fit lens models in each of the four input cosmologies, and refer to this as the systematic uncertainty that results from varying the input cosmological parameter values.

To quantify the degree to which cosmological parameter uncertainties affect the HFF strong lens models we begin by comparing the magnitude of the statistical and systematic uncertainties described above. We examine the average fractional uncertainty (statistical and systematic) as a function of the magnification for each of the six HFF clusters, and plot the results in Figure 1. It is crucial to establish that the scatter in magnification across the models with different input cosmologies are not simply the result of randomly sampling the statistical uncertainty. To do this we look at the distribution of magnification values at random positions on the sky across the full range of statistical models generated with each input cosmology for each cluster. Specifically, we select a random position and examine the magnification values of all pixels within a 9×9 pixel box ($4.5'' \times 4.5''$) centered on that position, and plot the distribution of all pixel magnification values in that region, across all statistical models in each of the four cosmologies.

In Figure 2 we show the results for a single random location in each HFF cluster field; the positions used here are just one randomly selected realization of ~ 100 such draws. The probability distribution of magnification values does change with the input cosmology – sometimes very dramatically and sometimes only weakly. The fact that the distribution of magnification values at a given position shifts *systematically* with input cosmology confirms that uncertainty in cosmological parameter values maps directly into a systematic uncertainty in lens models.

The relative scale of cosmological noise in the magnification maps for the HFF clusters are shown in Figure 3, where we plot the ratio of the fractional magnification uncertainties for each of the two cases – this is simply the ratio of the two solid lines plotted in each panel of Figure 1.

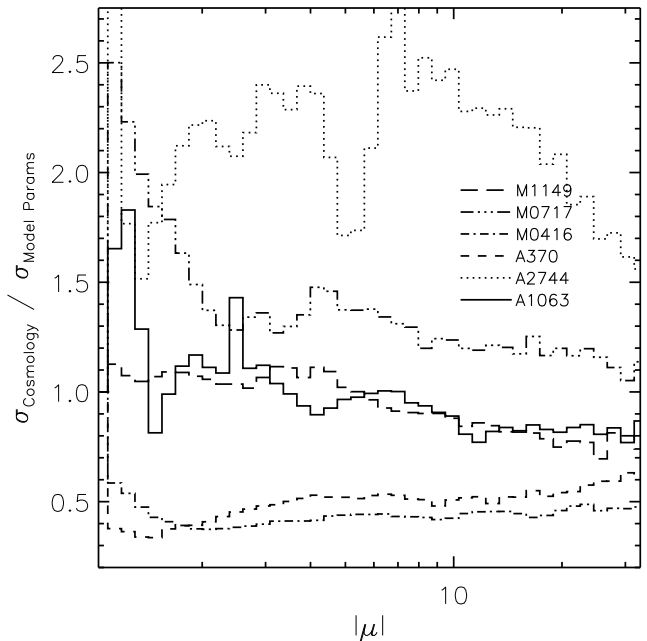


FIG. 3.— Ratio of median magnification uncertainties as a function of magnification that result from lens models with different input cosmologies vs. the statistical uncertainties from the strong lens models; each of the six HFF is plotted individually.

3.2. Impact of Cosmological Uncertainty When Scaling Lens Models to Arbitrary Source Redshifts

In addition to the modeling process, we must also assess the degree to which cosmological parameter uncertainties affect the ability to precisely scale lens model outputs to background sources at arbitrary redshifts. The magnification is computed directly from the maps for κ and γ (Schneider et al. 1992):

$$\mu = \frac{1}{(1 - \kappa)^2 - \gamma^2} \quad (5)$$

where both κ and γ scale proportionally to the distance term, d_{ls}/d_s . Here we assess the uncertainty in the distance ratio, d_{ls}/d_s , due to cosmological parameter uncertainty. Uncertainty in this distance ratio adds additional noise into magnification maps that are scaled to an arbitrary source redshift. We do this by calculating the fractional variation in the value of d_{ls}/d_s using the fiducial “concordance” parameter values as the control distance ratio – $d_{ls,0}/d_{s,0}$ – and compare this fiducial value to the distance ratio evaluated for other cosmological parameter values drawn from constraints in the literature (Table 1). This fractional uncertainty is computed as,

$$\frac{d_{ls}(z_s)/d_s(z_s)}{d_{ls,0}(z_s)/d_{s,0}(z_s)}. \quad (6)$$

We then apply the uncertainty in this distance ratio to the Sharon v2 κ and γ maps available from the HFF website to generate a range of scaled maps; from these maps we compute the RMS uncertainty in the magnification values for each pixel across these scaled maps and include the resulting fractional magnification uncertainty vs magnification in Figure 1. This uncertainty is sub-dominant to the other statistical and systematic uncertainties explored above, primarily because factors

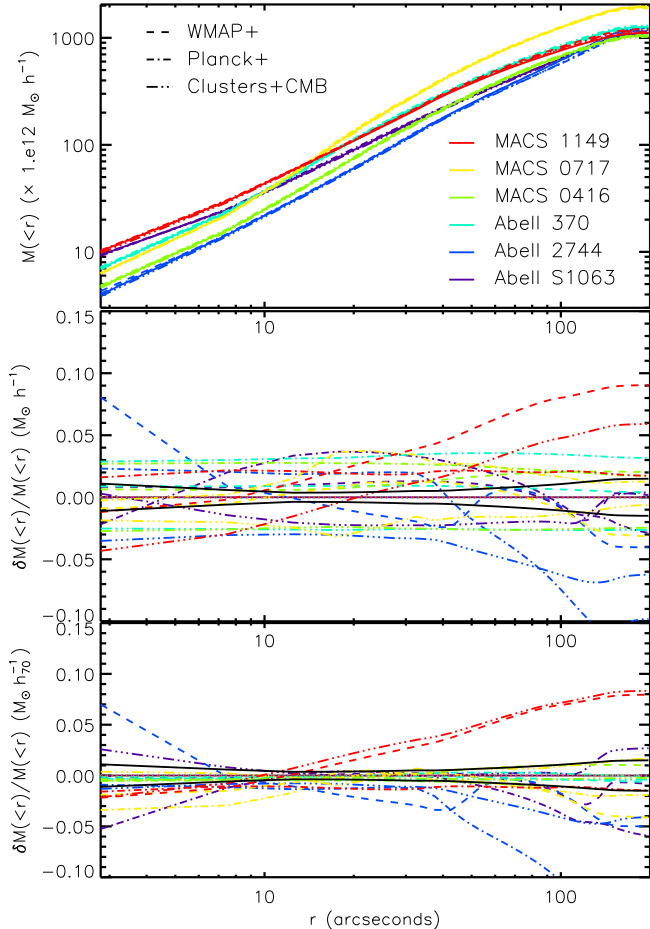


FIG. 4.— Enclosed mass as a function of radius and enclosed mass residuals (relative to the fiducial cosmology, see Table 1) for each of the six HFF clusters, plotted for the best fit mass maps in each of the four different cosmologies used here. The bottom two panels show the residuals in physical units (middle panel in units of $M_{\odot} h^{-1}$) and in common units normalized to the fiducial H_0 value (bottom panel in $M_{\odot} h_{70}^{-1}$). The residuals in the bottom panel most accurately reflect the cosmological uncertainties in the enclosed mass that result from lens model variations with cosmology. The statistical uncertainties in the enclosed mass are over-plotted as the solid black lines in the two residual panels, and are small ($<2\%$) at all radii; the cosmological uncertainties are everywhere as large or larger than the statistical uncertainties.

of H_0 cancel out when calculating the distance ratio, so that only the matter density, Ω_M matters, and because both of the relevant angular diameter distances, d_{ls} and d_s , change in the same way with changes in Ω_M .

3.3. Impact of Cosmological Uncertainty On Lensing Reconstructed Mass Maps

In this section we quantify the effect of varying the input cosmological parameters on the resulting mass maps for the lensing clusters. We take the output mass maps for the best fit lens model in each of the four cosmologies (Table 1) and measure the total enclosed mass vs. projected radius for each of the six HFF clusters, along with the residuals relative to the fiducial cosmology; the results are shown in Figure 4. We also estimate the statistical uncertainty in the mass profiles of the HFF clusters using the same lens models analyzed in previous sections. The $1-\sigma$ statistical uncertainty here is simply the half range of the value of the mass profile as computed from

the full range of statistical lens models drawn from the 68% confidence region of the MCMC chains. These statistical uncertainties are plotted in the middle and lower panels of Figure 4 along with the cosmological residuals.

Residuals in the enclosed mass (in physical units) are typically $\pm 5\%$ and remain fairly constant over two decades in projected radius. However, some component of these residuals are simply the result of the differences in the factor of h^{-1} that is multiplied into cosmological mass measurements. When we factor out this h^{-1} from the masses from different cosmologies the mass residuals shift to become smaller ($\sim 1-2\%$) at the radii where the best strong lensing constraints lie ($2'' \lesssim r \lesssim 20''$), with a few clusters having larger residuals at other radii.

One of the great strengths of strong lensing mass measurements is its precision, with typical statistical uncertainties of $\sim 1\%$ (Figure 4). Systematic cosmological mass residuals are as larger or larger ($\sim 1-2\%$) at radii where strong lensing constraints are typically used, but both statistical and cosmological uncertainties are very small in this region. While cluster mass measurements are not the primary science driver of the HFF, this remains one of the more powerful applications of strong lensing clusters (Comerford & Natarajan 2007; Oguri et al. 2009, 2012; Gralla et al. 2011; Merten et al. 2014), and it would be valuable for future analyses to consider the systematic uncertainty on cluster masses that are derived from strong lensing models.

4. DISCUSSION AND IMPLICATIONS

Varying the input cosmological parameters for the strong lens modeling process results in significant magnification uncertainties for all six of the HFF clusters. From Figures 1 and 3 we see that some of the clusters seem to be more strongly affected by cosmology than others. For example, Abell S1063, Abell 2744, MACS J0717, and MACS J1149 all have cosmological magnification uncertainties that are generally equal to or greater than the statistical uncertainties in the lens models, while Abell 370 and MACS J0416 have average cosmological magnification uncertainties that are only $\sim 40-60\%$ those the lens model parameter uncertainties. There are several possible drivers for increased uncertainty from cluster to cluster (e.g., number of constraints, the positional distribution of constraints, and availability of spectroscopic redshifts; Johnson et al. in prep), but we do note that clusters with a high fraction of arcs with spectroscopic redshifts have lower cosmological uncertainties compared to the statistical uncertainties. Specifically, 56% of the background sources for Abell 370 and 66% for MACS J0416 have spec-z's, whereas the background sources for the other four clusters all have between just 25-38% spec-z's (Table 3 in Johnson et al. 2014).

The broad results of our analysis here does strongly argue that it is not appropriate to assume that lens model parameter uncertainties dominate the error budget of precision strong lens models. There are already a number of early results using the first-pass HFF lens models to measure the intrinsic properties of distant background galaxies (Atek et al. 2014a,b; Bradley et al. 2014; Ishigaki et al. 2014; Kawamata et al. 2014; McLeod et al. 2014; Monna et al. 2014; Schmidt et al. 2014). Cosmological parameter uncertainty will fundamentally contribute at some level to the systematic

uncertainty in strong lens modeling, and our work here demonstrates that the cosmological contribution is likely at a level that cannot be ignored. Precisely quantifying these effects is certain to be sensitive to the modeling methodology; our results are specific to the lens models published in Johnson et al. (2014), and it would be up to individual lens model teams to fold in methods that allow for a range of input cosmologies. A true characterization of the magnification uncertainty marginalized over both cosmology and lens model parameters will require the investigation of cosmological parameter constraints in the MCMC minimization code. Looking ahead it is important that the strong lensing community continue the trend toward producing public lens models with comprehensive assessments of all relevant systematics, which certainly includes adopting methodologies that marginalize lens model uncertainties over a range of cosmological parameter values that span the current best-constraints.

One additional, somewhat tangential, implication of these results is that we are entering an era in which precision strong lensing maps of the HFF clusters might be used to provide independent constraints on geometric cosmological parameters. Jullo et al. (2010) first used the deflection constraints from multiply imaged sources in precision lens models to constrain cosmological parameter values, but it is not clear that the HFF lens models will necessarily be able to do better than previous work by Jullo et al. (2010).

5. CONCLUSIONS

Our results indicate that cosmological parameter uncertainties *do* contribute to the noise in magnification maps recovered for the HFF clusters at levels that are often comparable in magnitude to the statistical uncertainties in the lens models, and that they also impact strong lensing cluster masses at a similar level to the statistical modeling uncertainties. The prospect of producing competitive constraints on cosmological parameters from the deflection of light via strong lensing also is becoming interesting as the number of lenses with numerous constraints increases. In the new era of precision strong lens modeling, it is important that *all* source of systematic uncertainty be considered when totaling up the error budgets of strong lensing models for systems that are intended to be used as precision gravitational lenses – such as the HFF.

This work utilizes gravitational lensing models that were generated as a part of the HST Frontier Fields program conducted by STScI. STScI is operated by the Association of Universities for Research in Astronomy, Inc. under NASA contract NAS 5-26555. The lens models are hosted on the Mikulski Archive for Space Telescopes (MAST). The authors thank the referee, Dan Coe, for his thoughtful and helpful feedback. MBB acknowledges support from the NSF through grant AST-1009012 and from NASA through grant HST-GO-13639.01.

REFERENCES

- Atek, H., et al. 2014a, *ApJ*, 786, 60
 ——. 2014b, *ArXiv e-prints*, 1409.0512
 Bayliss, M. B., Johnson, T., Gladders, M. D., Sharon, K., & Oguri, M. 2014a, *ApJ*, 783, 41
 Bayliss, M. B., Rigby, J. R., Sharon, K., Wuyts, E., Florian, M., Gladders, M. D., Johnson, T., & Oguri, M. 2014b, *ApJ*, 790, 144
 Bradač, M., Schneider, P., Lombardi, M., & Erben, T. 2005, *A&A*, 437, 39
 Bradač, M., et al. 2009, *ApJ*, 706, 1201
 Bradley, L. D., et al. 2014, *ApJ*, 792, 76
 Coe, D., et al. 2013, *ApJ*, 762, 32
 Comerford, J. M., & Natarajan, P. 2007, *MNRAS*, 379, 190
 D’Aloisio, A., Natarajan, P., & Shapiro, P. R. 2014, *MNRAS*, 445, 3581
 Fukugita, M., Futamase, T., Kasai, M., & Turner, E. L. 1992, *ApJ*, 393, 3
 Gralla, M. B., et al. 2011, *ApJ*, 737, 74
 Hinshaw, G., et al. 2013, *ApJS*, 208, 19
 Ishigaki, M., Kawamata, R., Ouchi, M., Oguri, M., Shimasaku, K., & Ono, Y. 2014, *ArXiv e-prints*, 1408.6903
 Jauzac, M., et al. 2014a, *MNRAS*, 443, 1549
 ——. 2014b, *ArXiv e-prints*, 1409.8663
 Johnson, T. L., Sharon, K., Bayliss, M. B., Gladders, M. D., Coe, D., & Ebeling, H. 2014, *ApJ*, 797, 48
 Jullo, E., & Kneib, J.-P. 2009, *MNRAS*, 395, 1319
 Jullo, E., Kneib, J.-P., Limousin, M., Elíasdóttir, Á., Marshall, P. J., & Verdugo, T. 2007, *New Journal of Physics*, 9, 447
 Jullo, E., Natarajan, P., Kneib, J.-P., D’Aloisio, A., Limousin, M., Richard, J., & Schmid, C. 2010, *Science*, 329, 924
 Kawamata, R., Ishigaki, M., Shimasaku, K., Oguri, M., & Ouchi, M. 2014, *ArXiv e-prints*, 1410.1535
 Liesenborgs, J., De Rijcke, S., & Dejonghe, H. 2006, *MNRAS*, 367, 1209
 McCully, C., Keeton, C. R., Wong, K. C., & Zabludoff, A. I. 2014, *MNRAS*, 443, 3631
 McLeod, D. J., McLure, R. J., Dunlop, J. S., Robertson, B. E., Ellis, R. S., & Targett, T. T. 2014, *ArXiv e-prints*, 1412.1472
 Merten, J., Cacciato, M., Meneghetti, M., Mignone, C., & Bartelmann, M. 2009, *A&A*, 500, 681
 Merten, J., et al. 2014, *ArXiv e-prints*, 1404.1376
 Monna, A., et al. 2014, *MNRAS*, 438, 1417
 Oguri, M., Bayliss, M. B., Dahle, H., Sharon, K., Gladders, M. D., Natarajan, P., Hennawi, J. F., & Koester, B. P. 2012, *MNRAS*, 420, 3213
 Oguri, M., et al. 2009, *ApJ*, 699, 1038
 Planck Collaboration, et al. 2014, *A&A*, 571, A16
 Reichardt, C. L., et al. 2013, *ApJ*, 763, 127
 Richard, J., et al. 2014, *MNRAS*, 444, 268
 Schmidt, K. B., et al. 2014, *ApJ*, 782, L36
 Schneider, P., Ehlers, J., & Falco, E. E. 1992, *Gravitational Lenses*
 Sharon, K., Gladders, M. D., Rigby, J. R., Wuyts, E., Bayliss, M. B., Johnson, T. L., Florian, M. K., & Dahle, H. 2014, *ApJ*, 795, 50
 Sharon, K., Gladders, M. D., Rigby, J. R., Wuyts, E., Koester, B. P., Bayliss, M. B., & Barrientos, L. F. 2012, *ApJ*, 746, 161
 Tagore, A. S., & Keeton, C. R. 2014, *MNRAS*, 445, 694
 Zitrin, A., et al. 2014, *ArXiv e-prints*, 1411.1414